

RESEARCH ARTICLE

10.1002/2016JA023658

Key Points:

- The correlation between radiation belt electrons and solar wind/geomagnetic parameters as a function of μ and L^* has been unveiled
- Various solar wind/geomagnetic parameters correlate better with the enhancements of electron phase space density (PSD) than electron PSD
- Among all parameters investigated, AL index correlates the best with electron PSD enhancements, with correlation coefficients up to ~ 0.8

Correspondence to:

H. Zhao,
hong.zhao@lasp.colorado.edu

Citation:

Zhao, H., D. N. Baker, A. N. Jaynes, X. Li, S. R. Elkington, S. G. Kanekal, H. E. Spence, A. J. Boyd, C.-L. Huang, and C. Forsyth (2017), On the relation between radiation belt electrons and solar wind parameters/geomagnetic indices: Dependence on the first adiabatic invariant and L^* , *J. Geophys. Res. Space Physics*, 122, 1624–1642, doi:10.1002/2016JA023658.

Received 7 NOV 2016









Accepted 10 JAN 2017

Accepted article online 18 JAN 2017

Published online 8 FEB 2017

©2017. American Geophysical Union.
All Rights Reserved.

On the relation between radiation belt electrons and solar wind parameters/geomagnetic indices: Dependence on the first adiabatic invariant and L^*

H. Zhao¹ , D. N. Baker¹ , A. N. Jaynes¹ , X. Li¹ , S. R. Elkington¹ , S. G. Kanekal²,
H. E. Spence³ , A. J. Boyd⁴ , C.-L. Huang³, and C. Forsyth⁵ 

¹Laboratory for Atmospheric and Space Physics, University of Colorado, Boulder, Colorado, USA, ²Goddard Space Flight Center, NASA, Greenbelt, Maryland, USA, ³Institute for the Study of Earth, Oceans, and Space, University of New Hampshire, Durham, New Hampshire, USA, ⁴New Mexico Consortium, Los Alamos, New Mexico, USA, ⁵Department of Space and Climate Physics, Mullard Space Science Laboratory, University College London, London, UK

Abstract The relation between radiation belt electrons and solar wind/magnetospheric processes is of particular interest due to both scientific and practical needs. Though many studies have focused on this topic, electron data from Van Allen Probes with wide L shell coverage and fine energy resolution, for the first time, enabled this statistical study on the relation between radiation belt electrons and solar wind parameters/geomagnetic indices as a function of first adiabatic invariant μ and L^* . Good correlations between electron phase space density (PSD) and solar wind speed, southward $IMF B_z$, $SYM-H$, and AL indices are found over wide μ and L^* ranges, with higher correlation coefficients and shorter time lags for low- μ electrons than high- μ electrons; the anticorrelation between electron PSD and solar wind proton density is limited to high- μ electrons at high L^* . The solar wind dynamic pressure has dominantly positive correlation with low- μ electrons and negative correlation with high- μ electrons at different L^* . In addition, electron PSD enhancements also correlate well with various solar wind/geomagnetic parameters, and for most parameters this correlation is even better than that of electron PSD while the time lag is also much shorter. Among all parameters investigated, AL index is shown to correlate the best with electron PSD enhancements, with correlation coefficients up to ~ 0.8 for low- μ electrons (time lag ~ 0 day) and ~ 0.7 for high- μ electrons (time lag ~ 1 –2 days), suggesting the importance of seed and source populations provided by substorms in radiation belt electron PSD enhancements.

1. Introduction

Radiation belt electrons have attracted plenty of attention in the past due to both scientific interest and practical needs. Specifically, the influence of solar wind and magnetospheric processes on the dynamics of radiation belt electrons is of particular interest. Many studies have focused on the response of energetic electrons in the outer radiation belt to solar wind conditions, and it is widely accepted that energetic particles at geosynchronous Earth orbit (GEO) are modulated by the solar wind parameters [e.g., *Paulikas and Blake*, 1979; *Baker et al.*, 1979, 1986, 1990; *Blake et al.*, 1997; *Reeves*, 1998; *Mathie and Mann*, 2000; *O'Brien et al.*, 2001; *Li*, 2004; *Li et al.*, 2001, 2005; 2011; *Lyatsky and Khazanov*, 2008; *Borovsky and Denton*, 2009; *Reeves et al.*, 2011; *Boynnton et al.*, 2013; *Simms et al.*, 2016]. *Paulikas and Blake* [1979] analyzed energetic electron data from ATS-1, ATS-5, and ATS-6 spacecraft and found a pronounced positive correlation between the electron fluxes and solar wind speed. *Baker et al.* [1986], using data from the spectrometer for energetic electrons onboard 1979-053 and 1982-019 satellites, showed the good correlation between highly relativistic electrons and solar wind stream structures. *Blake et al.* [1997], based on measurements from 1994-026 and WIND spacecraft, conveyed a study of the correlation between relativistic electrons at GEO and properties of solar wind during a solar minimum period. Their results indicated that the relativistic electron enhancement is associated with solar wind speed increase along with solar wind density increase and southward turning of the IMF . Furthermore, *Li et al.* [2001], using a model based on the radial diffusion equation, quantitatively predicted the electron fluxes at GEO based on solar wind velocity and IMF , and a linear correlation of 0.9 between predicted and measured values was achieved for 1995–1996. The solar wind speed was found to be the most important factor in their prediction model. Recently, *Reeves et al.* [2011] revisited the relationship between relativistic electron fluxes at GEO and solar wind velocity using Los Alamos National Laboratory Geosynchronous Satellites (LANL-GEO) data from 1989 to 2010. Their results showed a pronounced triangle-shaped distribution

of electron fluxes versus solar wind speed, indicating that the radiation belt electron fluxes can be quite high at any solar wind speed. *Li et al.* [2011] emphasized that geomagnetic activity driven by a southward orientation of IMF is a necessary condition for MeV electron enhancements at GEO. *Boynnton et al.* [2013], using the Nonlinear AutoRegressive Moving Average with eXogenous inputs approach, studied the relation between electron fluxes at GEO and various solar wind parameters. Their results suggest that for lower energy electrons, the solar wind speed is the most controlling factor of electron fluxes at GEO, while for MeV electrons, the solar wind speed of 2 days before is the most important factor in electron fluxes. Most recently, *Wing et al.* [2016], using the information theory, investigated the solar wind driver of 1.8–3.5 MeV electrons at GEO. They showed that various solar wind parameters are causally related to 1.8–3.5 MeV electron fluxes at GEO, while among all parameters, the solar wind speed has shown to have the highest peak information transfer. These previous studies show the important role of solar wind on the dynamics of relativistic electrons at GEO.

There are also some statistical studies focusing on the electrons in the whole outer radiation belt and their relation to the solar wind parameters [e.g., *Li et al.*, 1997; *Baker et al.*, 1999; *Iles et al.*, 2002; *Vassiliadis et al.*, 2002; *Mann et al.*, 2004; *Rigler et al.*, 2007; *Li et al.*, 2009]. *Iles et al.* [2002], using >750 keV and >1 MeV electron data from two microsatellites, STRV-1a and 1b, which were in highly elliptical, near-equatorial orbits, studied the correlation between total relativistic electron content in the outer belt and solar wind and geomagnetic parameters during geomagnetic storms at the first 6 months of 1995. They found that the main requirements for relativistic electron enhancements are fast solar wind speed and fluctuating or southward IMF B_z . *Baker et al.* [2004] constructed the radiation belt electron content (RBC) index, which is a simple but robust estimate of total relativistic electrons in the outer radiation belt, and showed that the RBC is well correlated with solar wind speed and *Dst* index. *Mann et al.* [2004] investigated the correlations between ULF wave power, solar wind speed, and relativistic electron fluxes using data from ground magnetometers, LANL-GEO, and HEO satellites. They showed that high correlation exists between both solar wind speed and ULF power with MeV electron fluxes at *L* shells between 3.1 and 6.6, while electron fluxes respond first at higher *L* shells and subsequently at lower *L* shells.

On the other hand, magnetospheric processes have also been shown to be critical in radiation belt electron dynamics [e.g., *Baker et al.*, 1990; *Reeves*, 1998; *Reeves et al.*, 2003; *Li et al.*, 2009; *Zhao and Li*, 2013; *Jaynes et al.*, 2015]. Geomagnetic storms and substorms play essential roles in transport and acceleration of radiation belt electrons. *Reeves* [1998] studied 30 intense relativistic electron enhancement events at GEO from 1992 to 1995 and found rough correlation between maximum electron flux and minimum *Dst*, though geomagnetic storms are found to not necessarily cause flux enhancements. *Li et al.* [2009] analyzed total relativistic electron flux variations in the outer radiation belt during 18 storms from 1990 to 1991 and studied the statistical roles of storms and substorms on the radiation belt electron population. They found that the substorm activity is well correlated with the net increases of total electron fluxes in the outer belt. *Jaynes et al.* [2015], using data from Van Allen Probes, studied the importance of source and seed populations in radiation belt electron variations and showed the crucial role of substorms in radiation belt electron acceleration. Most recently, *Forsyth et al.* [2016] examined the total radiation belt electron content variations following substorms and showed the increases of total radiation belt electron content following substorms with a time lag of 1–3 days.

The roles of solar wind and magnetospheric processes on the radiation belt electrons have been extensively studied. However, due to the limit of observations, most previous studies only focused on relativistic electrons at GEO or on a very limited energy range. With the launch of Van Allen Probes, which provide clean radiation belt electron measurements in a wide *L* range with very fine energy resolution, we are able to study the correlation between radiation belt electrons and solar wind parameters/geomagnetic indices and its dependence on the energy of electrons and *L* shell for the first time. Also, the majority of previous studies only examined the correlation between various parameters and radiation belt electron fluxes. However, these studies cannot rule out the influence of adiabatic effect in their statistical analyses, which can greatly affect the measured electron fluxes during geomagnetic storms especially at higher *L* shells. In this paper, using data from the Magnetic Electron Ion Spectrometer (MagEIS) [*Blake et al.*, 2013] and the Relativistic Electron-Proton Telescope (REPT) [*Baker et al.*, 2012] instruments of the Energetic Particle, Composition, and Thermal Plasma (ECT) suites [*Spence et al.*, 2013] on the Van Allen Probes, we study the relation between radiation belt electron phase space density (PSD) and solar wind parameters/geomagnetic indices while focusing on its dependence on the first adiabatic invariant μ and L^* for a wide μ and L^* range. Using the electron PSD instead of fluxes, we exclude the influence of adiabatic effect, and thus, the actual effect of

solar wind/magnetospheric processes on radiation belt electrons can be appropriately highlighted. Besides the radiation belt electron PSD, we also show that the solar wind and magnetospheric processes play important roles in radiation belt electron acceleration by analyzing the relation between electron PSD enhancements and solar wind/geomagnetic parameters. Furthermore, the important role of substorms on radiation belt electron PSD enhancements and their prolonged effects are unveiled.

2. The Relation Between Radiation Belt Electron Phase Space Density (PSD) and Solar Wind Parameters/Geomagnetic Indices Based on the Van Allen Probes Measurements

Figure 1 shows the daily averaged fluxes of ~ 1 , 2.6, and 5.2 MeV electrons measured by the MagEIS and REPT instruments on Van Allen Probe – A, as well as the daily averaged solar wind speed, $IMF B_z$, $SYM-H$ index, and AL index during October 2012 to March 2016. High variability of outer radiation belt electrons can be seen from Figure 1, and the variation of electron fluxes is also L^* dependent and energy dependent. Clear correlation can be seen between radiation belt electron fluxes and geomagnetic indices, while solar wind speed and southward $IMF B_z$ also correlate roughly with electron fluxes. Figure 1 shows that the solar wind/magnetospheric processes have great effect on radiation belt electrons, and the correlation between them can be quite complicated.

Figure 2 shows the relation between daily averaged relativistic electron PSD and solar wind speed/ $SYM-H$ index, using data from Van Allen Probe – A from Oct 2012 to March 2016. In Figure 2, daily averaged $\mu = 1000$ MeV/G electron PSD at $L^* = 4.5$ are plotted versus daily averaged solar wind speed and $SYM-H$ index. Electrons with $\mu = 1000$ MeV/G at $L^* = 4.5$ have energies of ~ 1.2 MeV during geomagnetic quiet times. In this study, we examine the relation between solar wind/geomagnetic parameters and electron PSD instead of flux in order to exclude the adiabatic effects. Here spin-averaged electron flux data from REPT and MagEIS instruments are interpolated across electron energy to calculate the electron PSD with specific μ values, and the T89 model [Tsyganenko, 1989] is used to calculate the first adiabatic invariant μ and L^* (assuming locally mirroring particles). As can be seen from Figures 2a and 2b, the scatterplots of simultaneous electron PSD versus solar wind speed and $SYM-H$ index show the clear feature of a triangle-shaped distribution: the lower limit of electron PSD increases as solar wind speed increases and $SYM-H$ index decreases, while the higher limit of PSD is relatively constant. These results are similar to the scatterplot of daily averaged MeV electron fluxes at GEO versus solar wind speed shown in Reeves *et al.* [2011]. With a time lag of 2 days, as shown in Figures 2c and 2d, the correlation between electron PSD and solar wind speed/ $SYM-H$ index has been improved, and the scattering in Figures 2a and 2b has been reduced, similar to the scatterplot of daily averaged MeV electron fluxes at GEO versus solar wind speed shown in Figure 5 of Li *et al.* [2011]. Using data from Van Allen Probe – A, Figure 2 extends the previous results on the relation between relativistic electron fluxes and solar wind speed/ Dst index [e.g., Reeves *et al.*, 2011] to also show that daily averaged PSD of electrons with a fixed first adiabatic invariant μ at a fixed L^* still have clear correlation with solar wind speed/ $SYM-H$ index. In the rest of this section, enabled by the high-energy resolution electron data from Van Allen Probe – A, the dependence of such correlation on μ and L^* is investigated in detail, and the results are discussed.

2.1. Radiation Belt Electron PSD and Solar Wind Parameters

To investigate the effect of solar wind on the radiation belt electrons, correlation between radiation belt electron PSD and solar wind speed, southward $IMF B_z$ (defined as B_z when $B_z < 0$ and 0 when $B_z > 0$ in GSM coordinates), solar wind proton density, and solar wind dynamic pressure are examined as a function of first adiabatic invariant μ and L^* .

Figure 3 shows the correlation between the electron PSD with time lag and solar wind speed, southward $IMF B_z$, and solar wind proton density as a function of first adiabatic invariant μ and L^* . In this study, the linear correlation coefficients are calculated between various parameters and the logarithm of electron PSD or PSD enhancements (section 4). The correlation coefficients are calculated in μ and L^* bins, with 30μ bins ranging from 10 to 10,000 (evenly distributed in logarithm scale) and $30L^*$ bins ranging from 3 to 6 (evenly distributed). To ensure enough statistics, only bins with number of points greater than 100 are shown, and the time lags are only shown for bins with the absolute value of highest correlation coefficient greater

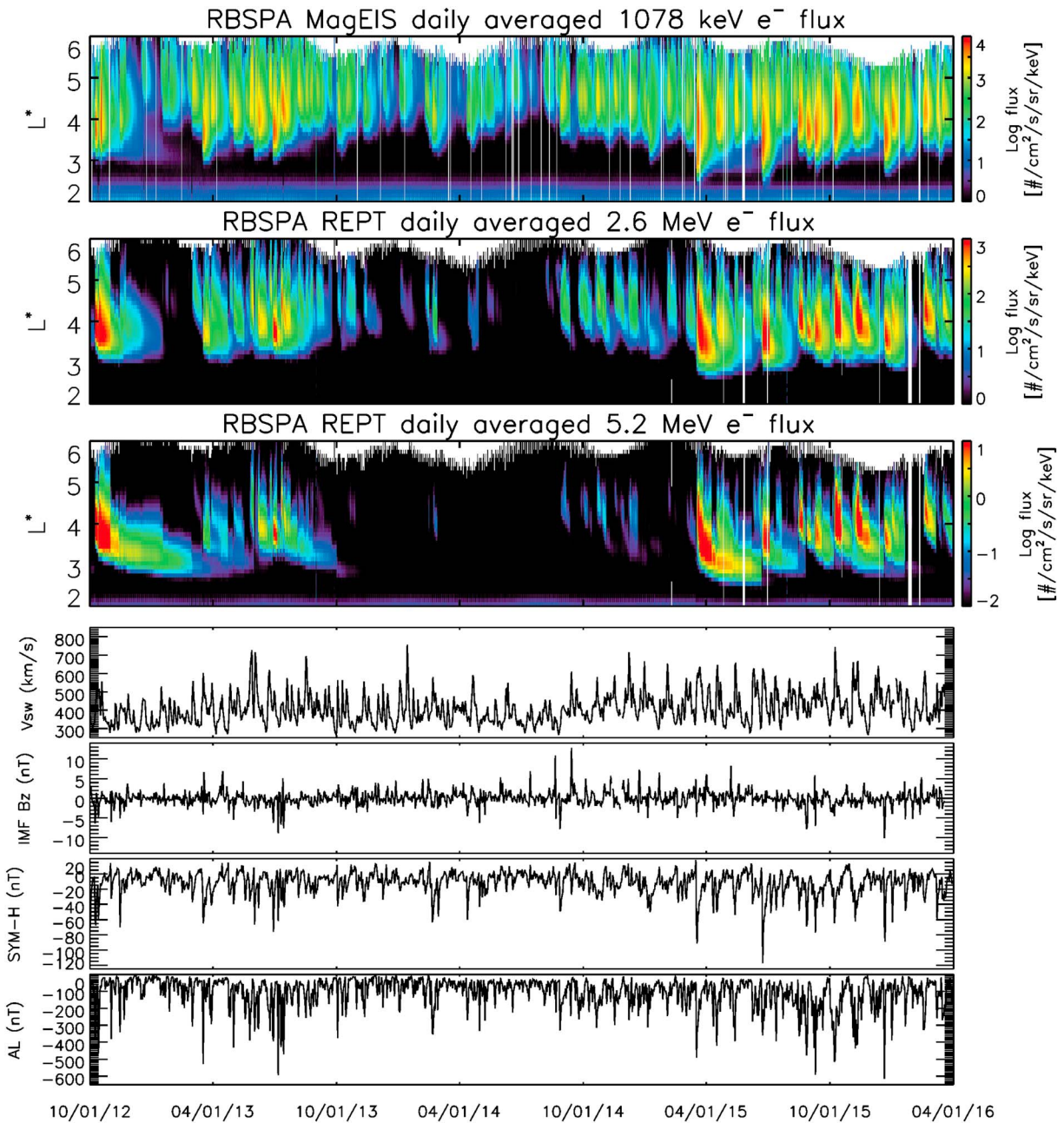


Figure 1. Daily averaged fluxes of 1078 keV, 2.6 MeV, and 5.2 MeV electrons, measured by MagEIS and REPT instruments on Van Allen Probe – A, along with daily averaged solar wind speed, $IMF B_z$, $SYM-H$ index, and AL index from October 2012 to March 2016.

than 0.2. Note that in this study, the range of color bars of correlation coefficients is different for solar wind speed/ $SYM-H/AL$ index and southward $IMF B_z$ /solar wind proton density/dynamic pressure since usually solar wind speed and geomagnetic indices have better correlation to the radiation belt electron PSD.

Evidently all three solar wind parameters have good correlation with radiation belt electron PSD with some time lags for some μ and L^* range. The solar wind speed and southward $IMF B_z$ have positive correlation with radiation belt electron PSD over wide μ and L^* ranges, while generally solar wind speed correlates better with the radiation belt electron PSD than southward $IMF B_z$; and comparing to high- μ electrons, low- μ electrons usually have better correlation with these parameters and shorter time delay. For high- μ electrons, the correlation between solar wind speed/southward $IMF B_z$ and electron PSD is stronger at higher L^* while weaker at lower L^* . For low- μ electrons, the good correlation can be observed over a much wider L^* range

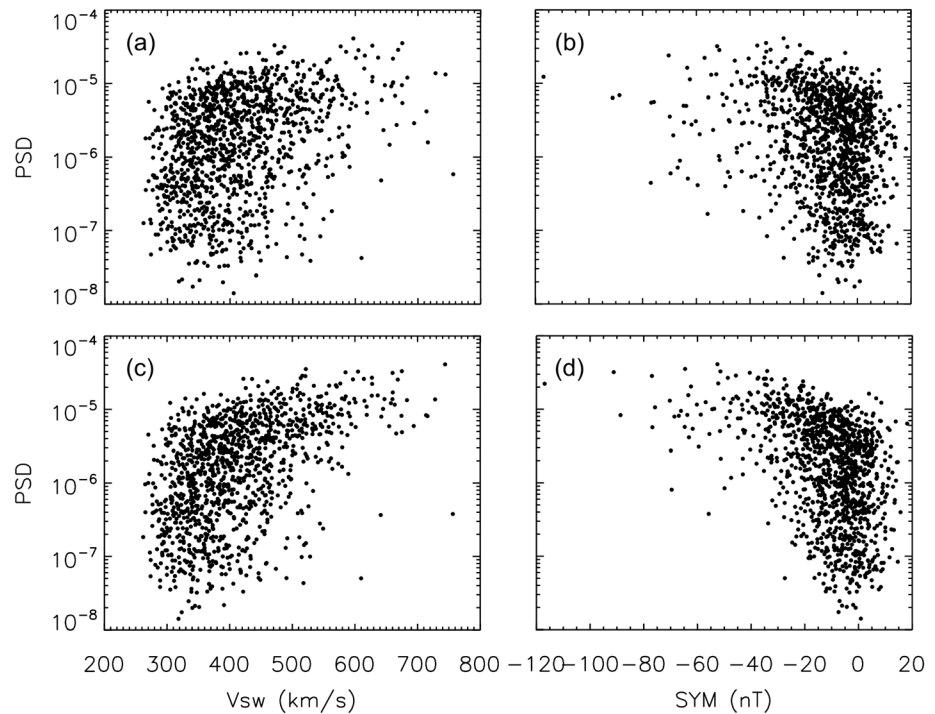


Figure 2. Daily averaged PSD of $\mu = 1000$ MeV/G electrons at $L^* = 4.5$ versus daily averaged (a and c) solar wind velocity (V_{sw}) and (b and d) $SYM-H$ index from October 2012 to March 2016, using data from Van Allen Probe – A and OMNIWeb. Figures 2a and 2b are the scatterplot of simultaneous electron PSD and $V_{sw}/SYM-H$ index; Figure 2c/2d is the scatterplot of PSD with time lag of 2 days versus $V_{sw}/SYM-H$ index.

(though not shown in Figure 3, down to $L^* \sim 2.5$). Generally the correlation coefficient peaks at lower L^* as μ gets smaller, suggesting that lower energy electrons are easier to be directly transported into lower L^* region, while high-energy electrons exhibit limited variations in the low L^* region, since Van Allen Probes era has been a relatively quiet time period. Low-energy electrons at high L^* are subject to influences from multiple magnetic processes, most of which have prompt effect on electrons, and thus, the correlation between daily averaged electron PSD and solar wind parameters is not high enough.

Also, the time lag to get the highest correlation coefficients gets longer as μ gets larger and L^* gets smaller. This indicates that the influence of solar wind speed and $IMF B_z$ to radiation belt electrons occurs faster for low- μ electrons and at higher L shells, which also agrees with previous studies [e.g., Mann et al., 2004]. Comparing the time lags, the radiation belt electrons usually respond faster to solar wind speed than southward $IMF B_z$, and the differences between them, as shown in Figure 3, is about 1 day. This shows that, comparing to southward $IMF B_z$, solar wind speed has a more prompt effect on the radiation belt electron PSD, though the underlying reason is not very clear.

Unlike the solar wind speed and southward $IMF B_z$, the solar wind proton density has a negative correlation with high- μ radiation belt electron PSD at high L^* . As the L^* gets lower and μ gets lower, the influence from solar wind proton density to the radiation belt electrons gets smaller; while as μ gets higher, the influence from solar wind proton density to the radiation belt electrons gets stronger. The time lags are usually 0–1 day, overall much shorter than solar wind speed and southward $IMF B_z$. This indicates that the loss associated with high solar wind proton density usually occurs fast and is limited to high L^* and high- μ electrons. One possible reason is that high solar wind proton density compresses the dayside magnetopause, causing relatively sudden loss through magnetopause shadowing, which affects high- μ electrons more at high L^* , as to be discussed further below.

Different from solar wind speed, southward $IMF B_z$, and solar wind proton density, the solar wind dynamic pressure has both positive and negative correlation with PSD of radiation belt electron with different μ at different L^* . Figure 4 shows the correlation between the solar wind dynamic pressure and radiation belt electron

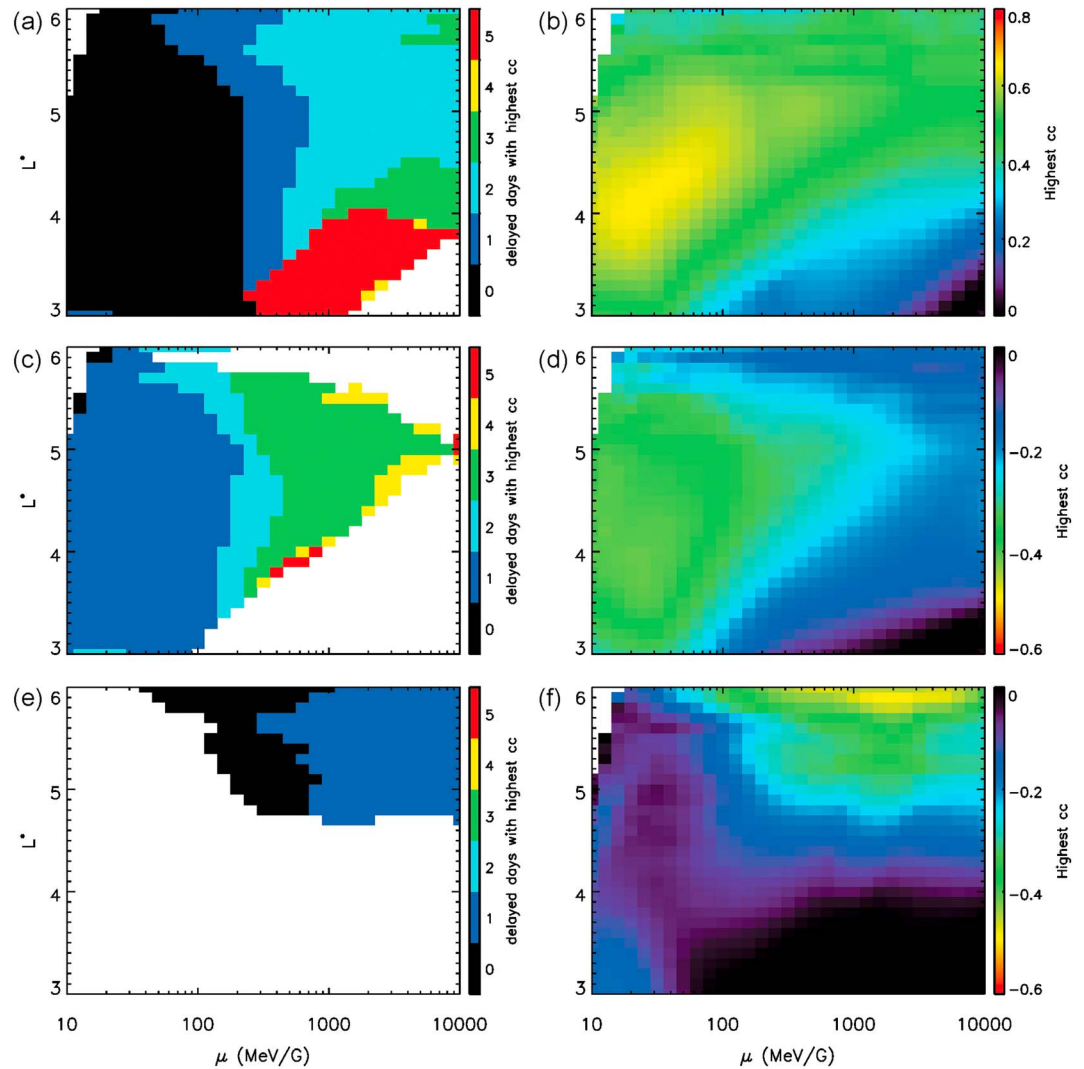


Figure 3. (left column) The time lags in days for the highest correlation coefficients between radiation belt electron PSD and (a) solar wind speed, (c) southward $IMF B_z$, and (e) solar wind proton density, as a function of the first adiabatic invariant μ and L^* ; (right column) The corresponding highest correlation coefficients between radiation belt electron PSD with time lag and (b) solar wind speed, (d) southward $IMF B_z$, and (f) solar wind proton density.

PSD as a function of μ and L^* . Figures 4a and 4b show the highest positive correlations between the solar wind dynamic pressure and radiation belt electron PSD with time lag, while Figures 4c and 4d show the greatest negative correlations. Similarly to Figure 3, the time lags are only shown for bins with absolute value of correlation coefficients greater than 0.2. Figure 4 clearly shows two different types of effects of solar wind dynamic pressure on radiation belt electrons. For low- μ electrons ($\mu < \sim 100\text{--}1000$ MeV/G), the dynamic pressure shows a dominantly positive correlation with electron PSD, with the correlation coefficient peaking at $L^* \sim 4\text{--}5$, and the time lag gets longer as μ gets larger. This may suggest the effect of radial transport of radiation belt electrons caused by ULF waves, which have shown to be well correlated with solar wind dynamic pressure and its variation [e.g., Liu *et al.*, 2010]. It is worth mentioning that the correlation between the dynamic pressure variation and electron PSD is also investigated and, though not shown here, the results are very similar to the results of dynamic pressure itself. This further confirms the effect of radial diffusion caused by solar wind dynamic pressure and its variation on the radiation belt electrons. For high- μ electrons at higher L^* , the dominant effect from solar wind dynamic pressure is the loss of relativistic electrons caused by magnetopause shadowing. As shown in Figures 4c and 4d, the negative correlation between solar wind dynamic pressure and electron PSD exists for $\mu > \sim 100$ MeV/G

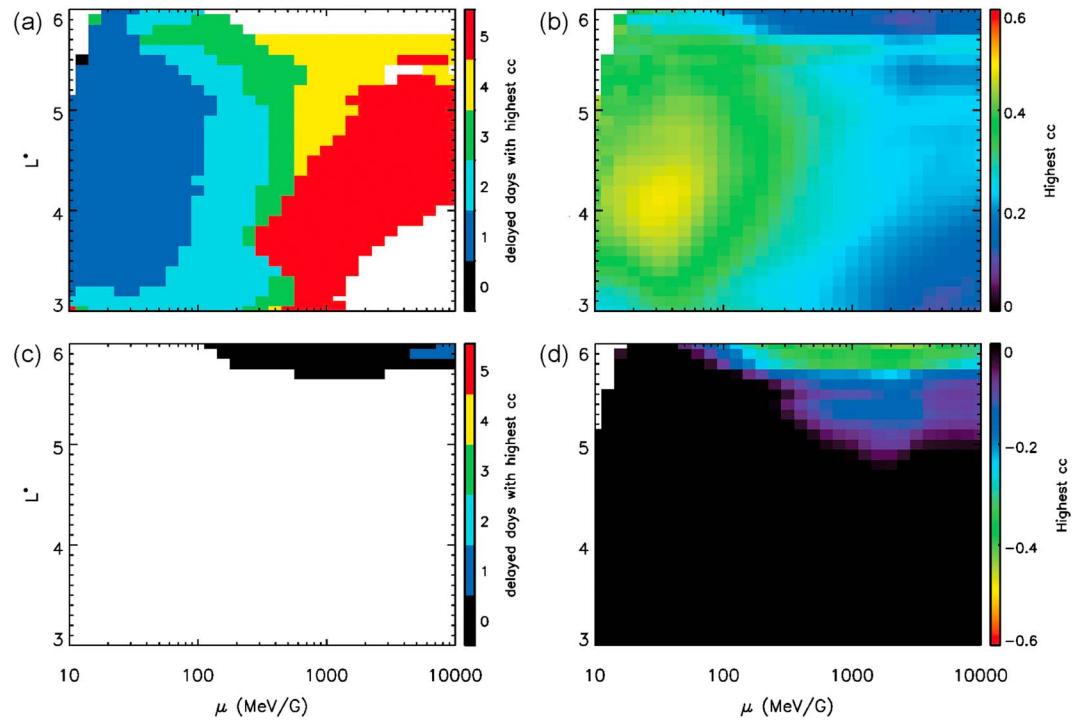


Figure 4. (a and c) The time lag in days of radiation belt electron PSD to get the highest correlation coefficients and (b and d) the corresponding (Figure 4b) positive/(Figure 4d) negative correlation coefficients between solar wind dynamic pressure and radiation belt electron PSD as a function of μ and L^* .

electrons at high L^* , and such correlation gradually decreases as μ gets smaller and L^* gets smaller. The negative effect of solar wind dynamic pressure on high- μ electrons at high L^* is almost simultaneous: the time lag is generally 0 day. This indicates the fast loss of radiation belt electrons due to magnetopause shadowing caused by high solar wind dynamic pressure.

2.2. Radiation Belt Electron PSD and Geomagnetic Indices

Besides solar wind parameters, geomagnetic indices have also been shown to correlate with radiation belt electrons [e.g., Reeves, 1998; Baker et al., 2004]. Identified by the decrease of the horizontal component of geomagnetic field at the Earth's surface, the geomagnetic storm is widely known to be able to produce enhancements or decreases of radiation belt electron fluxes [e.g., Reeves et al., 2003; Zhao and Li, 2013]. On the other hand, magnetospheric substorms have been shown to be important to radiation belt electron transport and acceleration as they provide the source and seed populations to the inner magnetosphere [e.g., Jaynes et al., 2015]. *SYM-H* index and *AL* index are commonly used as the proxy of geomagnetic storms and substorms, respectively. Figure 5 shows the plots similar to Figure 3 but for *SYM-H* and *AL* indices.

It can be seen from Figure 5 that both *SYM-H* and *AL* indices correlate well with radiation belt electron PSD over some μ and L^* range. Similar to the solar wind speed and southward *IMF B_z*, the correlation coefficient gets higher as μ gets lower: for high- μ electrons the PSD correlate well with *SYM-H* and *AL* indices only at higher L^* , while for low- μ electrons the PSD correlate well with geomagnetic indices over a much wider L^* range. Also, the time lag to get the highest correlation coefficient increases as μ increases and L^* decreases, which is very similar to the results for solar wind speed and southward *IMF B_z*. These results indicate that both geomagnetic storms and substorms have significant effect on radiation belt electrons, and the influence maximizes for low- μ electrons at lower L^* region and for high- μ electrons at higher L^* region.

The correlation between the *Dst* index (similar to *SYM-H* index but with time resolution of 1 h) and radiation belt electron fluxes has been extensively studied. *Tverskaya* [1986] investigated the relationship between the minimum *Dst* index during geomagnetic storms and the L of storm-injected relativistic electron peak fluxes (L_{max}) and showed that there is a linear correlation between the minimum *Dst* index and L_{max}^4 . *Tverskaya et al.* [2003],

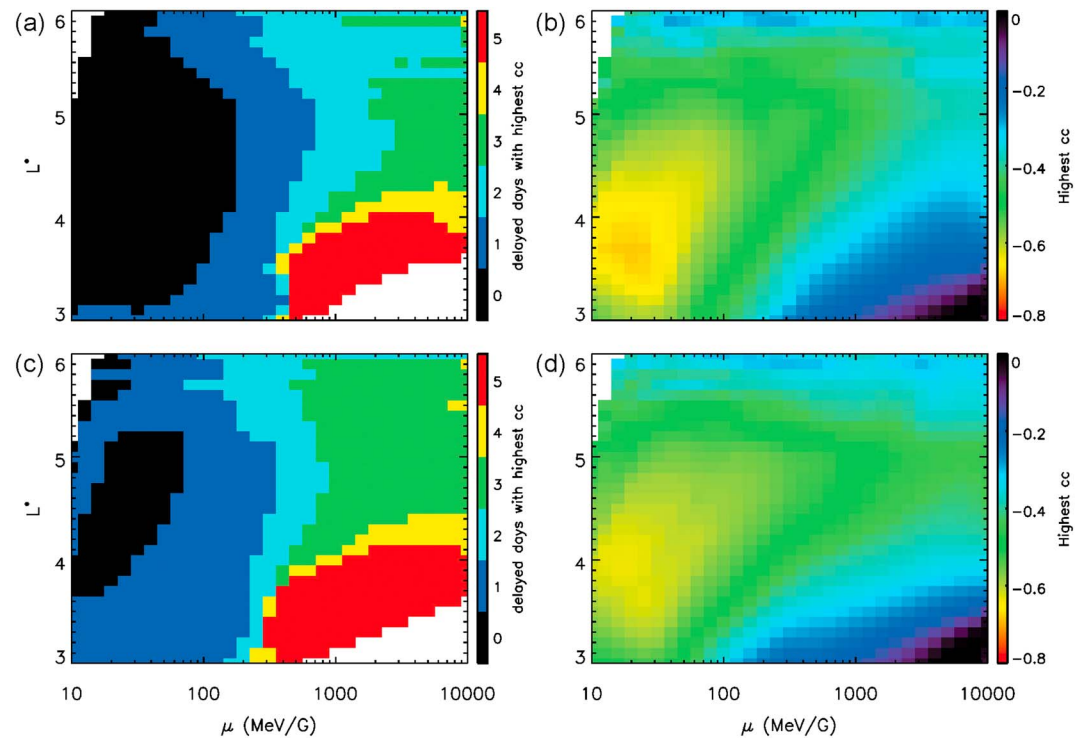


Figure 5. (left column) The time lag in days for the highest correlation coefficients between radiation belt electron PSD and (a) *SYM-H* and (c) *AL* indices; (right column) The corresponding highest correlation coefficients between radiation belt electron PSD with time lag and (b) *SYM-H* and (d) *AL* indices.

using data from SAMPEX, Polar, and HEO 1997-068 measurements, confirmed the correlation between the minimum *Dst* index and L_{max} during geomagnetic storms. Reeves [1998] studied 30 intense relativistic electron enhancement events at GEO from 1992 to 1995 and found rough correlation between maximum electron flux and minimum *Dst*, though geomagnetic storms are found to not necessarily cause flux enhancements. Zhao and Li [2013], using 2–6 MeV electron data from SAMPEX, showed that the *Dst* index is well correlated with the *L* shell on which the deepest penetration of MeV electrons occurred, and the maximum flux enhancements across the whole outer radiation belt were shown to be roughly correlated with the minimum *Dst* index during the geomagnetic storms (with the linear correlation coefficient of ~ 0.52). However, these previous studies cannot rule out the influence of adiabatic effect, which can greatly affect the electron fluxes during geomagnetic storms especially at higher *L* shells. Our study shows that, without the influence from adiabatic effect, the radiation belt electron PSD still correlate to the *SYM-H* index and thus the geomagnetic activity, and such correlation can be quite linear for low- μ electrons (with linear correlation coefficient up to ~ 0.7).

Comparing to solar wind parameters, we found that generally geomagnetic indices have better correlation with radiation belt electron PSD. As for the solar wind speed, the correlation coefficients are similar to those of *SYM-H* and *AL* indices; while for all other solar wind parameters, the correlation coefficients with radiation belt electron PSD are generally lower than those of *SYM-H* and *AL* indices (note that the color bars used for solar wind speed, *SYM-H*, and *AL* indices are different from those used for *IMF B_z*, solar wind proton density, and dynamic pressure). This indicates important roles of geomagnetic storms and substorms on radiation belt electron dynamics. It should be noted that Earth's magnetosphere has an organized way to respond to external driving forces [e.g., Li et al., 2003], while geomagnetic indices, such as *Dst* and *AL* indices, are well predicted based on multiple solar wind parameters [Temerin and Li, 2002, 2006; Li et al., 2007; Luo et al., 2013]. Here by correlating electron PSD with various parameters, we showed that as for a single parameter, geomagnetic indices have better correlation to radiation belt electron PAD than solar wind parameters, indicating a more direct relation between radiation belt electrons and geomagnetic activity than solar wind conditions.

Comparing *SYM-H* and *AL* indices, while their correlation coefficients to radiation belt electron PSD are similar, there are some differences in time lags: the time lag to get best correlation is a little bit longer for *AL* index than for *SYM-H* index. This may indicate that the substorms have prolonged effects on the radiation belt electrons, which will be shown in more detail in the next section.

3. Important Roles of Solar Wind Parameters/Geomagnetic Indices on the Radiation Belt Electron PSD Enhancements

In the previous section, we studied the correlation between solar wind parameters/geomagnetic indices, and radiation belt electron PSD as a function of μ and L^* using data from Van Allen Probe – A. The results show the pronounced triangle-shaped distributions between the solar wind parameters/geomagnetic indices and simultaneous radiation belt electron PSD; and with time lags, the correlation between the solar wind parameters/geomagnetic indices and radiation belt electron PSD has been improved.

Reeves *et al.* [2011] investigated the correlation between solar wind speed and radiation belt electron fluxes at GEO in detail. They showed that the triangle-shaped distribution is mainly caused by the long-lasting nature of relativistic electrons under relatively quiet solar wind/geomagnetic conditions. Thus, the solar wind parameters/geomagnetic indices may have more significant effect on radiation belt electron flux variations rather than the absolute flux levels. In addition, various physical processes have influence on radiation belt electron acceleration, loss, and transport. Investigating the relation between various solar wind parameters/geomagnetic indices and radiation belt electron PSD variations can provide valuable information on the underlying source and loss processes and their effect on relativistic electrons in a statistical sense.

In this section, we investigate the correlation between solar wind parameters/geomagnetic indices and radiation belt electron PSD variations. The electron PSD variations here are defined as the differences between daily averaged electron PSD. We further separate PSD variations into two subsets, enhancements and decreases, and mainly focus on the electron PSD enhancements in this section.

Figure 6 shows the scatterplots between daily averaged solar wind speed, southward *IMF B_z*, *SYM-H* and *AL* indices, and $\mu = 1000$ MeV/G electron PSD enhancements at $L^* = 4.5$ (corresponding to electrons with energy ~ 1.2 MeV during geomagnetic quiet times). Here the electron PSD enhancement at $t = \tau$ is calculated as $dPSD(t = \tau) = PSD(t = \tau) - PSD(t = \tau - 1)$, and only those data with $dPSD > 0$ are plotted in Figure 6 versus daily averaged solar wind/magnetospheric parameters of $t = \tau - 1$ day. It is evident that the PSD enhancements of $\mu = 1000$ MeV/G electrons at $L^* = 4.5$ correlate well with all four parameters. Especially, *AL* index has a nearly linear correlation with electron PSD enhancements with correlation coefficient of -0.64 , corresponding to an $r^2 \sim 0.4$, which suggests that $\sim 40\%$ of variability in electron PSD enhancements can be explained by *AL* index. This indicates that the solar wind speed, *IMF B_z*, geomagnetic storms, and substorms have significant effect on radiation belt electron acceleration at the center of outer radiation belt.

The correlation between various parameters and radiation belt electron PSD as a function of μ and L^* has been investigated in the previous section, which suggests the effect of solar wind/magnetospheric processes on the radiation belt electrons as a function of μ and L^* . However, as the acceleration and loss of electrons are mixed together and especially the long-lasting nature of high-energy electrons is ignored, the correlations between various parameters and electron PSD are not ideal to show the effect of different physical processes. In this section, by focusing on the electron PSD enhancements, the source processes of radiation belt electrons are emphasized, and the influence of various solar wind/magnetospheric parameters to radiation belt electron acceleration is unveiled. As Figure 6 shows, by focusing on the PSD enhancements, the correlation between different parameters and radiation belt electrons has also been improved. In the rest of this section, we will focus on the correlation between electron PSD enhancements and various solar wind/magnetospheric parameters as a function of μ and L^* . Similarly, the time lags between PSD enhancements and various parameters are also taken into consideration. The electron PSD enhancement at $t = \tau$ day is defined as $dPSD(t = \tau) = PSD(t = \tau) - PSD(t = \tau - 1)$ and is correlated with daily averaged solar wind/magnetospheric parameters of $t = \tau - dt$, where dt is the time lag in days between PSD enhancements and various parameters. The time lags of electron PSD enhancements to get the best correlation with various solar wind/magnetospheric parameters and the corresponding highest correlation coefficients are plotted, and the underlying physical processes are speculated.

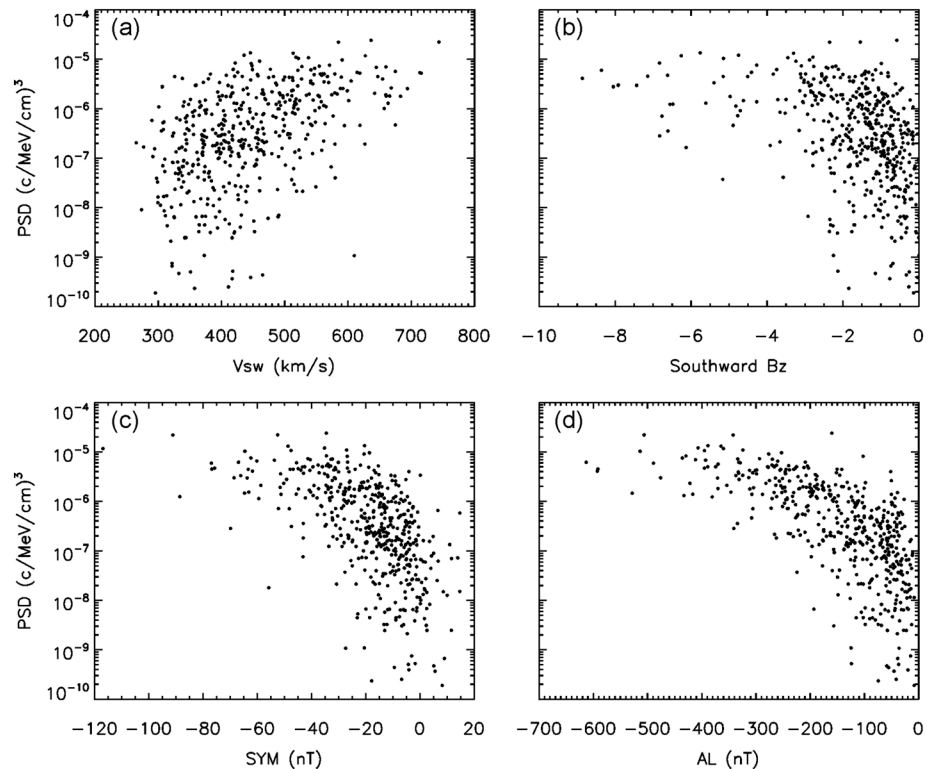


Figure 6. The scatterplot of (a) solar wind speed, (b) southward $IMF B_z$, (c) $SYM-H$ index, and (d) AL index with the $\mu = 1000$ MeV/G electron PSD enhancements at $L^* = 4.5$.

3.1. Radiation Belt Electron PSD Enhancements and Solar Wind Parameters

Figure 7 shows the correlation of radiation belt electron PSD enhancements with solar wind speed, southward $IMF B_z$, and solar wind dynamic pressure as a function of μ and L^* . Comparing Figure 7 to Figure 3, we find that the correlation between solar wind speed and radiation belt electron PSD or PSD enhancements is quite similar, indicating that the solar wind speed not only correlates well with the electron PSD but also plays an important role in radiation belt electron PSD enhancements. The correlation of southward $IMF B_z$ to radiation belt electron PSD enhancements is generally much higher than that to electron PSD, with correlation coefficients up to ~ 0.6 ($r^2 \sim 0.36$); the situation is similar for the solar wind dynamic pressure comparing with Figure 4.

Especially, for high- μ electrons, the correlation between PSD enhancements and solar wind parameters is stronger than that between PSD and solar wind parameters, indicating a significant effect of solar wind conditions on high- μ electron acceleration. The trend that the correlation coefficients are higher for low- μ electrons at relatively lower L^* and for high- μ electrons at higher L^* still holds. This also suggests the important role of solar wind conditions in the penetration of radiation belt electrons into the low L^* region.

As for the time lag, it is also clear from Figure 7 that overall the time lag increases as the μ increases, consistent with results from the previous section. Generally, for radiation belt electron PSD enhancements the time lag corresponding to the best correlation to solar wind parameters is about 0–2 days, which is much shorter than that of electron PSD, indicating the prompt enhancements of radiation belt electron PSD in response to solar wind conditions.

Good correlation between radiation belt electron PSD enhancements and various solar wind parameters indicates the important roles of solar wind on the radiation belt electron acceleration. It is well known that the radiation belt electrons are subjected to influences from various transport, acceleration, and loss mechanisms. Commonly, the radiation belt electrons can be energized by the adiabatic effect, inward radial diffusion, and local wave heating. Due to the change of geomagnetic field configuration and the conservation of three adiabatic invariants, radiation belt electrons can move inward/outward and get energized/de-energized.

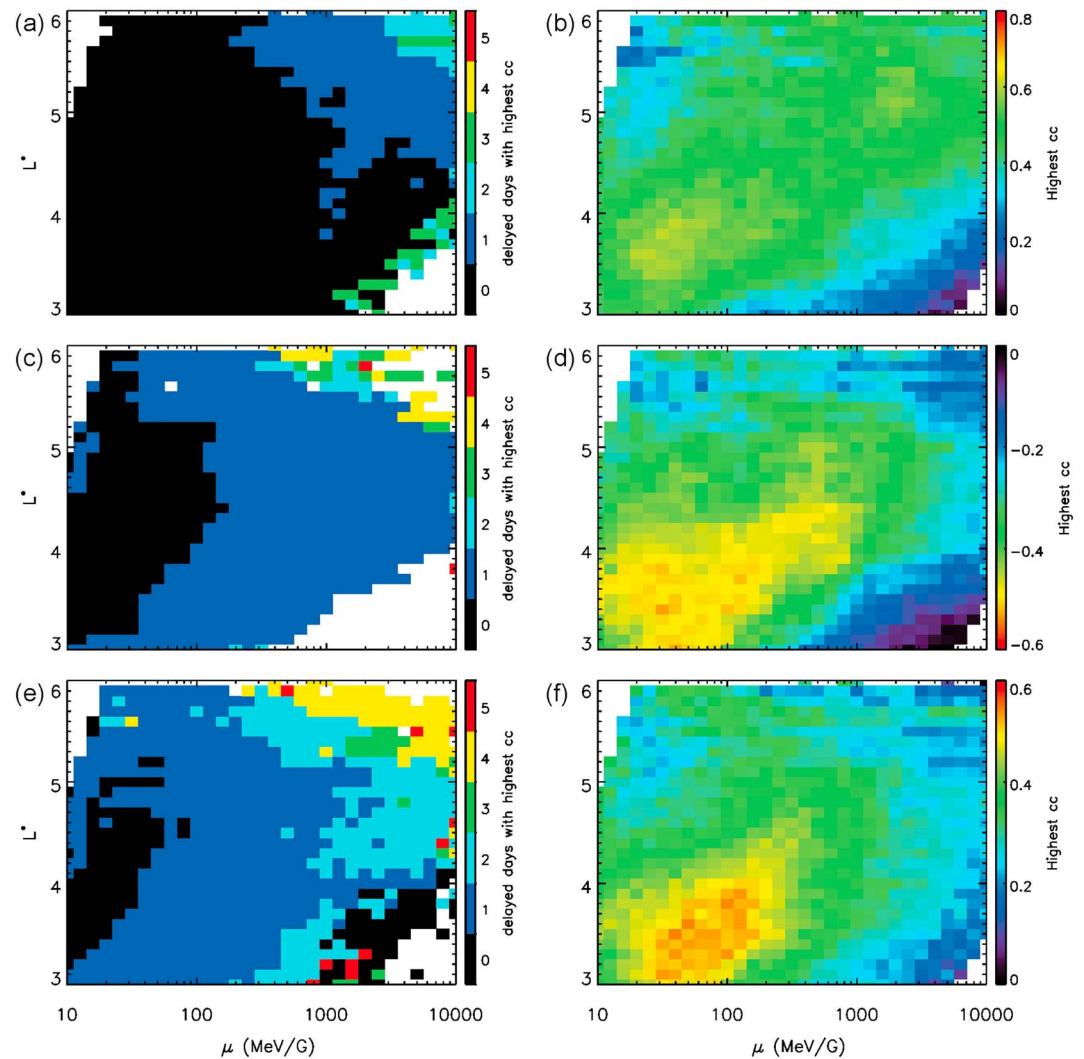


Figure 7. (a, c, and e) The time lags of radiation belt electron PSD enhancements to get the best correlation with solar wind parameters; (b, d, and f) The corresponding highest correlation coefficients, as a function of μ and L^* . The solar wind and IMF parameters from top to bottom are as follows: (Figures 7a and 7b) solar wind speed, (Figures 7c and 7d) southward IMF B_z , and (Figures 7e and 7f) solar wind dynamic pressure.

Thus, the adiabatic effect can cause the observed flux variations; however, it is not a real source or loss process since the electron PSD remains unchanged. In most previous studies on the correlation between solar wind/magnetospheric parameters and radiation belt electrons, the electron fluxes were used, in this way, however, the adiabatic effect cannot be ruled out, and the underlying physical processes cannot be appropriately unveiled. In this study, using the electron PSD instead of fluxes, we exclude the influence of adiabatic effect and thus focus on the real source/loss processes in the radiation belt.

The radiation belt electrons can be energized by moving radially inward through inward radial diffusion while conserving the first two adiabatic invariants. It is well known that ULF waves can cause radial diffusion of radiation belt electrons and thus is a major contributor to the radiation belt electron acceleration [e.g., Baker et al., 1998a, 1998b]. The solar wind velocity has been shown to be closely related to the ULF waves in the magnetosphere [e.g., Mathie and Mann, 2001; Mann et al., 2004; Claudepierre et al., 2008]. As shown in our study, the solar wind speed is positively correlated with electron PSD enhancements for electrons of a wide μ and L^* range. The correlation coefficient is up to ~ 0.7 , which indicates that $\sim 50\%$ of variations in the electron PSD can be explained by the solar wind speed variation, while the correlation coefficient is generally greater than ~ 0.4 for a large μ and L^* range. Also, the time lag to get the best correlation

increases as μ increases, which is consistent with the inward radial diffusion process as the electrons gradually moving inward and gaining energy. The positive correlation between solar wind speed and radiation belt electron PSD enhancements indicates the important role of radial diffusion on the radiation belt electrons which affect electrons with a large μ range and across the whole radiation belt. Similarly, the positive correlation between solar wind dynamic pressure and radiation belt electron PSD enhancements, especially for low- μ electrons, suggests the importance of radial diffusion in accelerating electrons in the center of outer radiation belt, as the solar wind dynamic pressure and pressure variations have shown to be well correlated to the ULF waves in the magnetosphere.

The correlation between southward $IMF B_z$ and electron PSD/PSD enhancements is not as high as that of solar wind speed. The highest correlation coefficient between southward $IMF B_z$ and electron PSD enhancements is ~ 0.5 at $L^* \sim 3-4$ for low- μ electrons; while at high L shells, the correlation coefficient is quite low. This result is consistent with the results from *Wing et al.* [2016], which showed that at GEO 1.8–3.5 MeV electron fluxes overall are not well correlated with southward $IMF B_z$ using information theory, and the correlation is weaker than that of solar wind speed, number density, and dynamic pressure. The energy transfer from solar wind to magnetosphere is more efficient under southward $IMF B_z$. However, the response from radiation belt electron PSD enhancements is not very well correlated with southward $IMF B_z$. This may be because the energy transferred from solar wind to magnetosphere influence radiation belt electrons in many different ways: as a result not only those source processes enhance but some loss processes also get stronger. With the competition between source and loss processes, the radiation belt electrons respond to southward $IMF B_z$ in a more complicated way.

On the other hand, though not shown here, the correlation between solar wind proton density/dynamic pressure and radiation belt electron PSD decreases is also investigated. The correlation, though still present, is generally weaker than the correlations between solar wind proton density/dynamic pressure and radiation belt electron PSD. This may be caused by the fast loss of radiation belt electrons in response to the variations of solar wind number density and dynamic pressure, which are much less than 1 day and cannot be well captured by daily averaged variations.

3.2. Radiation Belt Electron PSD Enhancements and Geomagnetic Indices

Figure 8 shows the time lags and corresponding highest correlation coefficients between radiation belt electron PSD enhancements and $SYM-H/AL$ index.

Comparing to Figure 5, it is clear that overall the geomagnetic indices correlate much better to radiation belt electron PSD enhancements than to radiation belt electron PSD. Notably, the correlation between AL index and high- μ electron PSD enhancements can reach almost 0.7 ($r^2 \sim 0.5$), which shows the important role of substorms in the radiation belt high-energy electron PSD enhancements. Still, the response of radiation belt electron PSD enhancements to geomagnetic storms/substorms is quite prompt, particularly for the low- μ electrons, as the time lag corresponding to the highest correlation coefficients is generally only 0–1 days.

It is well known that geomagnetic storms have complicated effect on radiation belt electrons, which can produce net increase, decrease, or little change of radiation belt electron fluxes almost regardless of storm intensity [e.g., *Reeves et al.*, 2003; *Turner et al.*, 2015; *Anderson et al.*, 2015]. On the other hand, *Zhao and Li* [2013] showed that most moderate and intense geomagnetic storms can always cause some flux enhancements of 2–6 MeV electrons at some L shells, though the total electron content of the radiation belt may increase or decrease, while the magnitude of maximum flux enhancement during moderate or intense geomagnetic storms is roughly correlated with the storm intensity (with $cc = 0.52$). In this subsection, by investigating the correlation between radiation belt electron PSD enhancements and $SYM-H$ index, we further confirmed the results of *Zhao and Li* [2013] by excluding the adiabatic effect and showed the correlation between PSD enhancements and storm intensity. For high- μ electrons, the correlation coefficient can be up to ~ 0.6 , which is consistent with results from *Zhao and Li* [2013]; while for low- μ electrons, the correlation coefficient can be up to ~ 0.8 , indicating significant effect of storms on the low- μ electron enhancements in the radiation belt. The high correlation coefficients and short time lag between low- μ electron PSD enhancements and storm intensity suggest the importance of magnetospheric convection to low- μ electrons in the radiation belt [e.g., *Korth et al.*, 1999; *Zhao et al.*, 2015, 2016].

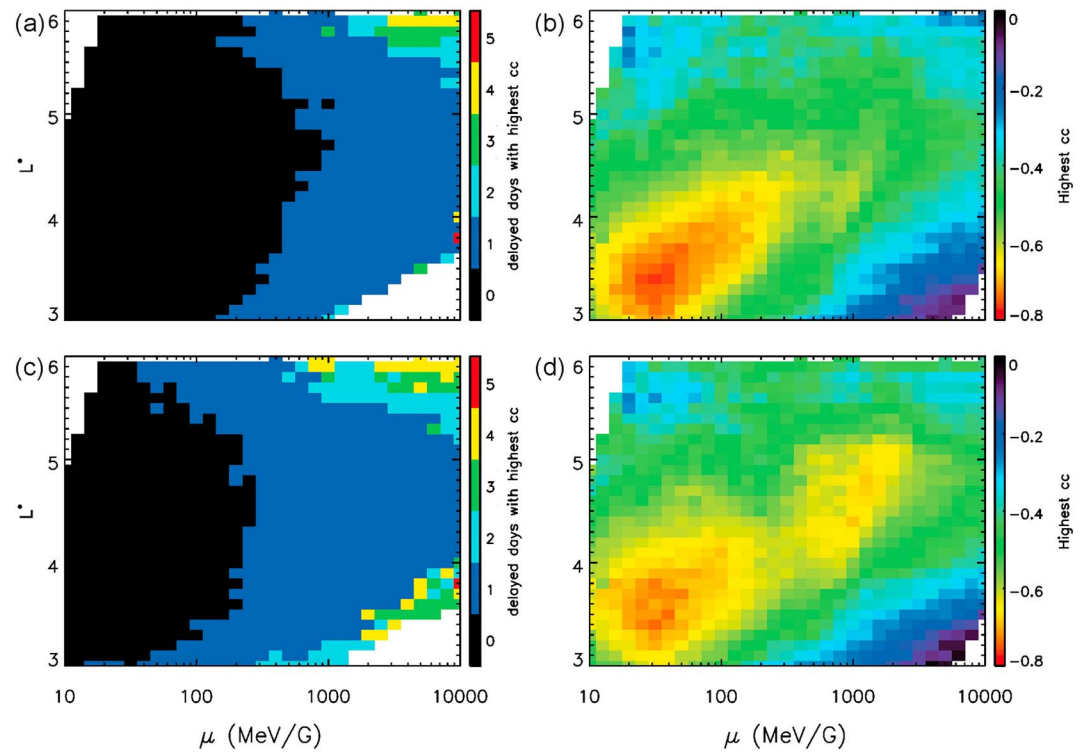


Figure 8. (a and c) The time lag of radiation belt electron PSD enhancements corresponding to the best correlation coefficient with geomagnetic indices, and (b and d) the corresponding highest correlation coefficients, as a function of μ and L^* . Figures 8a and 8b are for *SYM-H* index, and Figures 8c and 8d are for *AL* index.

The important role of magnetospheric substorms on the radiation belt electron acceleration has also been shown in many previous studies. Substorms provide source and seed populations for the radiation belt electrons, which are essential for the radiation belt electron acceleration [e.g., Jaynes *et al.*, 2015; Boyd *et al.*, 2016]. Our results show that, for low- μ electrons, *AL* index has good correlation with electron PSD enhancements with correlation coefficient up to ~ 0.8 , suggesting the importance of substorm injections of low-energy electrons; for high- μ electrons, *AL* index has the best correlation among all solar wind/magnetospheric parameters we investigated, and the correlation coefficient can be up to ~ 0.7 even for $\mu = 1000$ MeV/G electrons, which corresponds to electrons with energies of \sim MeV at GEO and even higher energies in the center of outer radiation belt. Such a good correlation indicates the important and direct role of substorms on the radiation belt electron acceleration. Substorms provide both source (\sim tens of keV) and seed (\sim hundreds of keV) populations to the inner magnetosphere. The high correlation between substorm intensity and low- μ electron PSD enhancements suggest the direct transport of low- μ electrons as a result of substorm injections; while on the other hand, the seed population can be further accelerated to higher energies by the VLF waves generated by the source population, and the high correlation between substorm intensity, and high- μ electron PSD enhancements support this scenario and the relatively longer time lag for high- μ electrons also suggest that the energization processes take on average 1 day to energize seed populations into MeV electrons.

The time lag of electron PSD enhancements to get the best correlation with *AL* index is slightly longer than that with *SYM-H* index and increases as the μ increases. To show more details about the response of radiation belt electrons to *AL* index as a function of time lag, Figure 9 shows the correlation coefficients between electron PSD enhancements and *AL* index as a function of time delay for three μ values, 100, 300, and 1000 MeV/G, at $L^* = 4.5$. It is clear that the correlation coefficient for $\mu = 100$ MeV/G electrons and *AL* index is highest with no time lag and gradually decreases as the time lag increases; while for $\mu = 300$ and 1000 MeV/G electrons, the maximum correlation coefficient appears at time lag of 1 day. Especially, for $\mu = 1000$ MeV/G electrons, the correlation coefficient remains relatively high (~ 0.5) even with a time lag of 2 days, comparable to the correlation

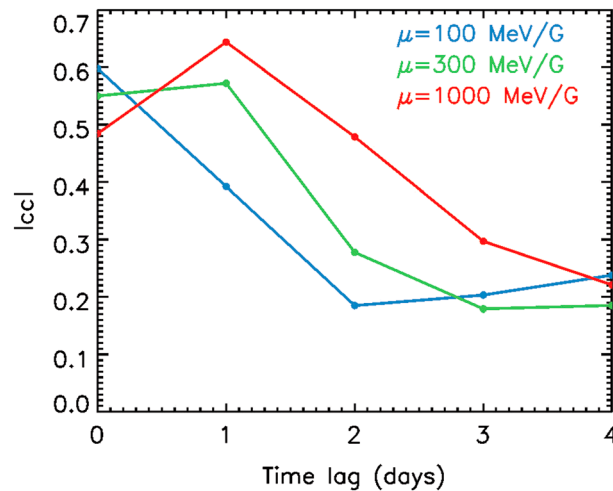


Figure 9. The absolute values of correlation coefficients between electron PSD enhancements at $L^* = 4.5$ and AL index as a function of time lag in days for $\mu = 100, 300$, and 1000 MeV/G.

with no time lag. This indicates that the influence from substorms to the higher energy electrons in the radiation belt is prolonged: lower energy electrons can be directly injected into the inner magnetosphere by substorms, while those newly injected or previously existing electrons need to be energized through wave-particle interactions caused by waves generated by source populations provided by substorms to higher energies. As Figure 9 shows, this energization processes take some time for high- μ electrons, with the peak enhancement occurs with a time lag of 1 day while significant enhancement can still be expected with a time lag of 2 days.

It is worth to mention that the magnetospheric activities are often nonlinear as pointed out by *Boynton et al.* [2011]. While comparing to the linear correlation analysis, the mutual information (MI) can better indicate the relation between two parameters in a nonlinear system. Though not shown here, we have examined the relation between relativistic electron PSD/PSD enhancements at different L^* for electrons with different μ values and various solar wind/geomagnetic parameters using MI. The results show very similar trends between MI and linear correlation analysis which indicate the response of relativistic electrons to various solar wind/magnetospheric parameters are dominated by linear dynamics, consistent with results from *Boynton et al.* [2013] and *Wing et al.* [2016].

In this study, we investigate the details of correlation between various solar wind/magnetospheric parameters and radiation belt electron PSD/PSD enhancements. The results show different effects of different parameters on radiation belt electrons as a function of μ and L^* , and the underlying physical processes are speculated. Moreover, the correlation shown in this study can further benefit future studies on modeling the radiation belt electron fluxes. Many models of relativistic electron fluxes in GEO have been established [e.g., *Baker et al.*, 1990; *Koons and Gorney*, 1991; *Li et al.*, 2001; *Turner and Li*, 2008]. However, limited model has been constructed regarding the radiation belt electron fluxes as a function of electron energy and L shell, which is very important for both scientific interest and practical needs. Our results on the correlation between various solar wind/magnetospheric parameters and radiation belt electron PSD/PSD enhancements as a function of μ and L^* provide valuable information on the most effective parameters in radiation belt electron dynamics and will benefit future work on the construction of radiation belt electron flux models.

4. Discussion

4.1. The Radiation Belt Electron Content Index and Solar Wind Parameters/Geomagnetic Indices

Baker et al. [2004] introduced the radiation belt electron content (RBC) index, which is an integral of radiation belt electron fluxes over the whole outer radiation belt region and a representative of total number of electrons in the outer radiation belt. Using data from SAMPEX satellite, they showed that the RBC index can be used as a good proxy of total radiation belt electrons and also correlates well with solar wind speed and the *Dst* index. Here using a quantity that is similar to RBC index in *Baker et al.* [2004] as a measurement of number of electrons with fixed first adiabatic invariant in the outer radiation belt, we also investigate the correlation between the total electrons in the outer radiation belt and solar wind parameters/geomagnetic indices. Specifically, we focus on the dependence of correlation on the first adiabatic invariant and time lag. Using the method similar to the one used in *Zhao et al.* [2015], the number of electrons with fixed μ is calculated by integrating electron distribution function between $L^* = 3$ and $L^* = 6$, assuming the number

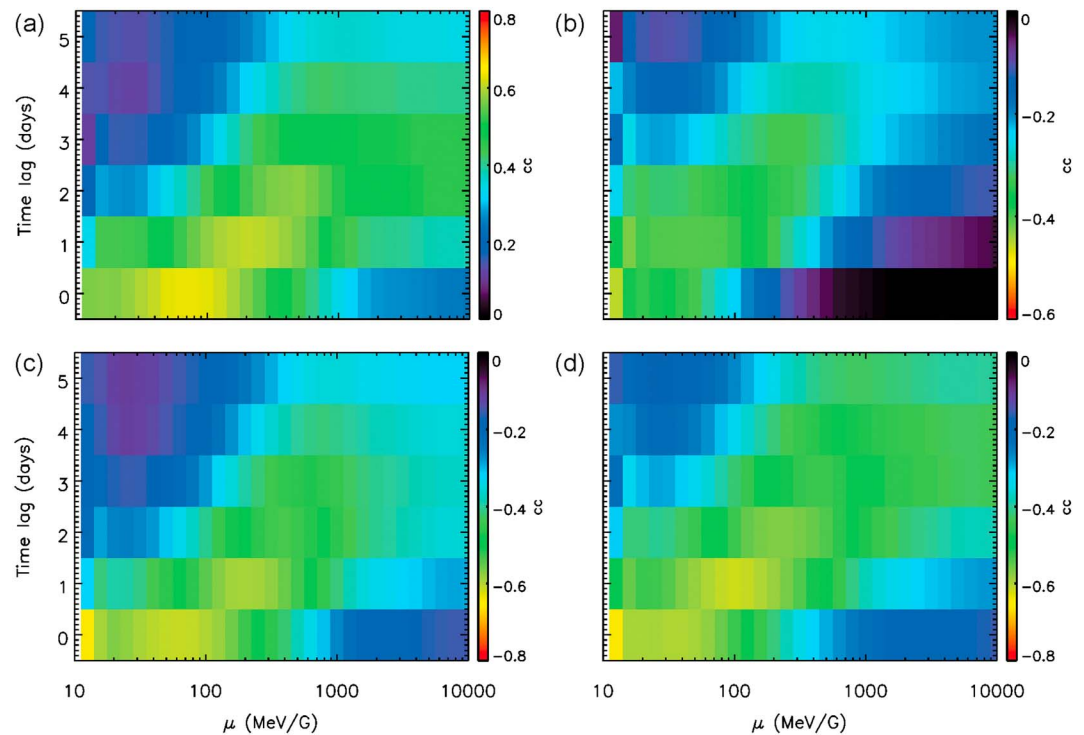


Figure 10. The correlation coefficients between radiation belt electron content (RBC) index and (a) solar wind speed, (b) southward $IMF B_z$, (c) $SYM-H$ index, and (d) AL index, as a function of μ and time lag.

density of electrons with fixed μ at a fixed L shell is constant. For simplicity we still call this quantity the RBC index in the rest of this section.

Figures 10 and 11 show the correlation coefficients of daily averaged RBC index and RBC index enhancements versus solar wind speed, southward $IMF B_z$, $SYM-H$, and AL indices as a function of μ and time lag. It is clear from Figure 10 that solar wind speed, southward $IMF B_z$, $SYM-H$ index, and AL index have good correlation with the RBC index across a wide range of μ . Overall, for low- μ electrons RBC index correlates better with solar wind parameters/geomagnetic indices; as μ gets higher, the highest correlation coefficient gets lower, and the time lag to get the highest correlation coefficient gets longer. Among these four parameters, still, AL index has the overall highest correlation coefficients to RBC index, which indicates the important role of substorms in accelerating radiation belt electron population.

Figure 11 shows that, similar to the electron PSD enhancements, good correlation also exists between RBC index enhancements and solar wind parameters/geomagnetic indices. The trend still holds that as μ gets higher, the time lag for highest correlation coefficient gets longer. While different from the correlation between RBC index and solar wind parameters/geomagnetic indices, Figure 11 shows that the correlation between enhancements of total number of electrons and different parameters peaks at $\mu \sim 200\text{--}2000$ MeV/G instead of lower μ values. One possible reason is that at higher L region, at which electrons contribute to the RBC index the most, the response of low- μ electrons to the solar wind parameters/geomagnetic storms and substorms is faster than 1 day, and thus, the statistics are not very good for daily averaged data. Still, AL index has the highest correlation coefficient with the enhancements of RBC index, showing that the substorm is a very important source for radiation belt electrons and plays an important role in the increase in total number of electrons in the outer radiation belt.

4.2. The Correlation Between Radiation Belt Electron PSD/PSD Enhancements and Solar Wind-Magnetosphere Coupling Function

The correlations between radiation belt electron PSD/PSD enhancements and solar wind-magnetosphere coupling are also investigated using the universal solar wind-magnetosphere coupling function. The universal solar wind-magnetosphere coupling function, constructed by *Newell et al.* [2007] by examining the

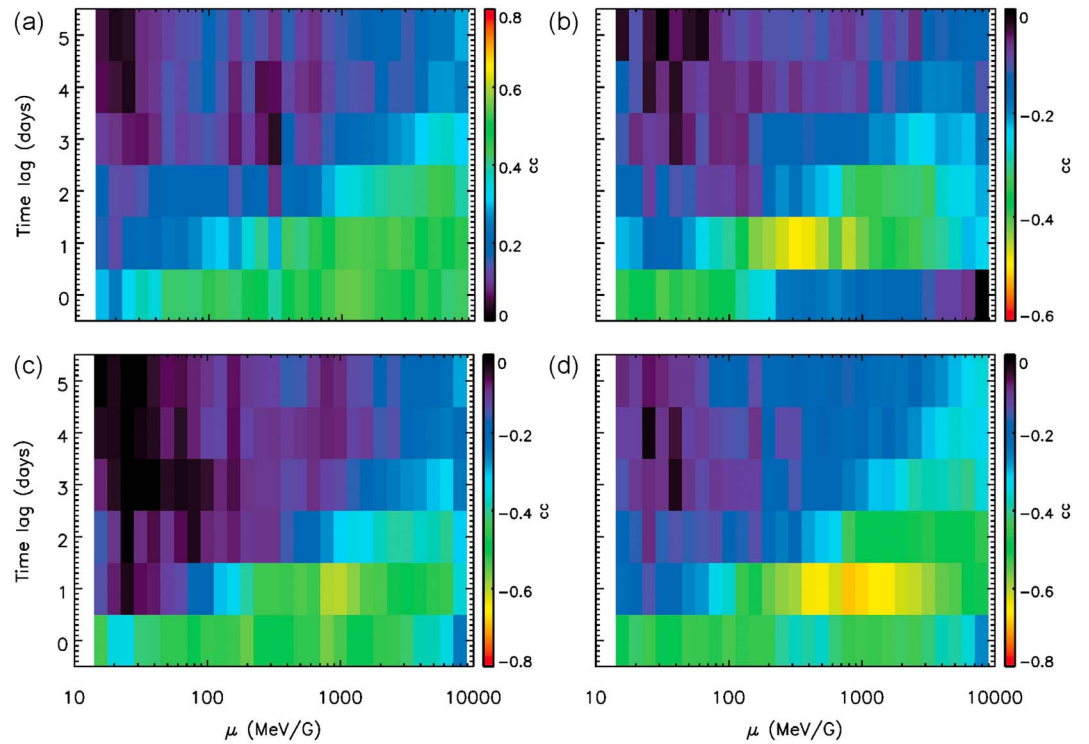


Figure 11. The correlation coefficients between RBC index enhancements and (a) solar wind speed, (b) southward *IMF* B_z , (c) *SYM-H* index, and (d) *AL* index, as a function of μ and time lag.

interaction between solar wind and magnetosphere, represents the rate of magnetic flux opened at the magnetopause and is shown to be well correlated with various geomagnetic indices. It can be calculated as

$$\frac{d\Phi_{MP}}{dt} = v^3 B_T^2 \sin^3\left(\frac{\theta_c}{2}\right)$$

where $\frac{d\Phi_{MP}}{dt}$ represents the rates of magnetopause magnetic flux opening, v is the solar wind speed, B_T is the perpendicular component of *IMF*, and θ_c is the *IMF* clock angle. Figure 12 shows the time lag and highest correlation coefficients between the radiation belt electron PSD/PSD enhancements and universal solar wind-magnetosphere coupling function as a function of μ and L^* . It is evident from Figure 12 that the universal solar wind-magnetosphere coupling function correlates well with both radiation belt electron PSD and PSD enhancements, with correlation coefficients up to ~ 0.65 ($r^2 \sim 0.42$), while the dependence on μ and L^* is similar to that of solar wind speed and southward *IMF* B_z . The results suggest that the solar wind-magnetosphere coupling and energy transfer have great influence on radiation belt electrons.

5. Summary

In this paper, using data from Van Allen Probe – A, we investigate the correlation of various solar wind parameters and geomagnetic indices with the radiation belt electron PSD and PSD enhancements. With proper orbit, wide energy coverage, and high energy resolution of Van Allen Probes, the dependence of the correlation on the first adiabatic invariant and L^* is unveiled. The main conclusions include

1. Both solar wind parameters and geomagnetic indices are shown to be correlated with radiation belt electron PSD with some time lag over some μ and L^* range. The correlations between radiation belt electron PSD and solar wind speed, southward *IMF* B_z , *SYM-H*, and *AL* indices are shown to be relatively high over large μ and L^* ranges with higher correlation coefficients for low- μ electrons, while the correlation coefficient generally peaks at lower L^* for lower- μ electrons and at higher L^* for higher- μ electrons. The anticorrelation between electron PSD and solar wind proton density is shown to be limited to high- μ electrons at high L^* region, suggesting the effect of magnetopause shadowing. The solar wind dynamic pressure has shown to have both positive and negative correlation with radiation belt electrons with

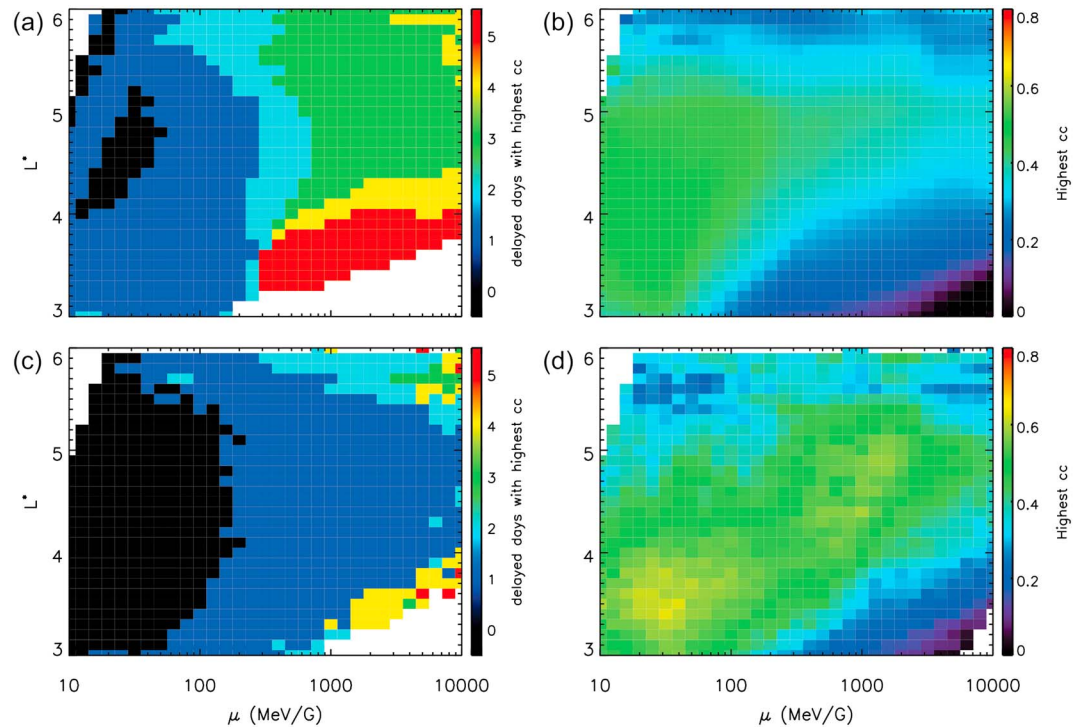


Figure 12. (left column) The time lag of (a) radiation belt electron PSD/(c) electron PSD enhancements corresponding to the highest correlation coefficient with universal solar wind-magnetosphere coupling function, and (right column) the corresponding highest correlation coefficients, as a function of μ and L^* .

different μ at different L^* . For low- μ electrons ($\mu < \sim 100\text{--}1000$ MeV/G), the dynamic pressure shows a dominantly positive correlation with electron PSD, suggesting the effect of radial transport of radiation belt electrons caused by ULF waves, which are well correlated with solar wind dynamic pressure and its variation; for high- μ electrons at higher L^* , the dominant effect from solar wind dynamic pressure is the loss of relativistic electrons caused by magnetopause shadowing.

2. The time lag to get the best correlation between electron PSD and solar wind speed, dynamic pressure (positive correlation), and geomagnetic indices generally increases as μ increases and L^* decreases, which is consistent with previous studies. This suggests the direct transport of low- μ electrons by convection/substorm injection while preexisting or newly injected electrons are gradually energized to higher energies by various source processes, e.g., inward radial diffusion and local wave heating.
3. Both solar wind parameters and geomagnetic indices are shown to be correlated with radiation belt electron PSD enhancements, while for most parameters the correlation to radiation belt electron PSD enhancements is better than that to electron PSD, indicating the direct correlation between various parameters and source processes in the radiation belt. Also, the time lag for radiation belt electron PSD enhancements, usually 0–2 days, is much shorter than that for electron PSD. These results indicate the important roles and prompt effects of solar wind and magnetospheric processes to radiation belt electron acceleration.
4. Among all solar wind parameters and geomagnetic indices investigated, *AL* index is shown to have the best correlation with the radiation belt electron PSD and PSD enhancements. For low- μ electrons, the correlation coefficients between *AL* index and PSD enhancement are up to ~ 0.8 ($r^2 \sim 0.6$) and time lag to get the best correlation is generally 0 day, indicating the direct transport of low- μ electrons through substorm injections; for high- μ electrons, the correlation coefficients are up to ~ 0.7 ($r^2 \sim 0.5$), and as μ increases, the time lag also increases, suggesting the important roles of source and seed populations injected by substorms in radiation belt electron PSD enhancements. The seed population can be accelerated to higher energies by waves generated by the source population, and our results suggest that on statistical sense the peak enhancement of electron PSD occurs with a time lag of 1 day after the magnetospheric substorm while significant enhancement can still be expected with a time lag of 2 days.

Acknowledgments

Van Allen Probes MagEIS and REPT data used in this paper are available from the ECT Science Operations and Data Center (<http://www.rbsp-ect.lanl.gov>). Solar wind data and geomagnetic indices are provided by OMNIWeb (<http://omniweb.gsfc.nasa.gov/>).

References

- Anderson, B. R., R. M. Millan, G. D. Reeves, and R. H. W. Friedel (2015), Acceleration and loss of relativistic electrons during small geomagnetic storms, *Geophys. Res. Lett.*, *42*, 10,113–10,119, doi:10.1002/2015GL066376.
- Baker, D. N., R. D. Belian, P. R. Higbie, and E. W. Hones Jr. (1979), High-energy magnetospheric protons and their dependence on geomagnetic and interplanetary conditions, *J. Geophys. Res.*, *84*, 7138–7154, doi:10.1029/JA084iA12p07138.
- Baker, D. N., J. B. Blake, R. W. Klebesadel, and P. R. Higbie (1986), Highly relativistic electrons in the Earth's outer magnetosphere: 1. Lifetimes and temporal history 1979–1984, *J. Geophys. Res.*, *91*, 4265–4276, doi:10.1029/JA091iA04p04265.
- Baker, D. N., R. L. McPherron, T. E. Cayton, and R. W. Klebesadel (1990), Linear prediction filter analysis of relativistic electron properties at 6.6 RE, *J. Geophys. Res.*, *95*, 15,133–15,140, doi:10.1029/JA095iA09p15133.
- Baker, D. N., et al. (1998a), A strong CME-related magnetic cloud interaction with the Earth's magnetosphere: ISTP observations of rapid relativistic electron acceleration on May 15, 1997, *Geophys. Res. Lett.*, *25*, 2975–2978, doi:10.1029/98GL01134.
- Baker, D. N., et al. (1998b), Coronal mass ejections, magnetic clouds, and relativistic magnetospheric electron events: ISTP, *J. Geophys. Res.*, *103*, 17,279–17,291, doi:10.1029/97JA03329.
- Baker, D. N., S. G. Kanekal, T. I. Pulkkinen, and J. B. Blake (1999), Equinoctial and solstitial averages of magnetospheric relativistic electrons: A strong semiannual modulation, *Geophys. Res. Lett.*, *26*, 3193–3196, doi:10.1029/1999GL003638.
- Baker, D. N., S. G. Kanekal, and J. B. Blake (2004), Characterizing the Earth's outer Van Allen zone using a radiation belt content index, *Space Weather*, *2*, S02003, doi:10.1029/2003SW000026.
- Baker, D. N., et al. (2012), The Relativistic Electron-Proton Telescope (REPT) instrument on board the Radiation Belt Storm Probes (RBSPP) spacecraft: Characterization of Earth's radiation belt high-energy particle populations, *Space Sci. Rev.*, *179*, 337–381, doi:10.1007/s11214-012-9950-9.
- Blake, J. B., D. N. Baker, N. Turner, K. W. Ogilvie, and R. P. Lepping (1997), Correlation of changes in the outer-zone relativistic electron population with upstream solar wind and magnetic field measurements, *Geophys. Res. Lett.*, *24*, 927–929, doi:10.1029/97GL00859.
- Blake, J. B., et al. (2013), The magnetic electron ion spectrometer (MagEIS) instruments aboard the radiation belt storm probes (RBSPP) spacecraft, *Space Sci. Rev.*, *179*, 383–421, doi:10.1007/s11214-013-9991-8.
- Borovsky, J. E., and M. H. Denton (2009), Relativistic-electron dropouts and recovery: A superposed epoch study of the magnetosphere and the solar wind, *J. Geophys. Res.*, *114*, A02201, doi:10.1029/2008JA013128.
- Boyd, A. J., H. E. Spence, C.-L. Huang, G. D. Reeves, D. N. Baker, D. L. Turner, S. G. Claudepierre, J. F. Fennell, J. B. Blake, and Y. Y. Shprits (2016), Statistical properties of the radiation belt seed population, *J. Geophys. Res. Space Physics*, *121*, 7636–7646, doi:10.1002/2016JA022652.
- Boynnton, R. J., M. A. Balikhin, S. A. Billings, H. L. Wei, and N. Ganushkina (2011), Using the NARMAX OLS-ERR algorithm to obtain the most influential coupling functions that affect the evolution of the magnetosphere, *J. Geophys. Res.*, *116*, A05218, doi:10.1029/2010JA015505.
- Boynnton, R. J., M. A. Balikhin, S. A. Billings, G. D. Reeves, N. Ganushkina, M. Gedalin, O. A. Amariutei, J. E. Borovsky, and S. N. Walker (2013), The analysis of electron fluxes at geosynchronous orbit employing a NARMAX approach, *J. Geophys. Res. Space Physics*, *118*, 1500–1513, doi:10.1002/jgra.50192.
- Claudepierre, S. G., S. R. Elkington, and M. Wiltberger (2008), Solar wind driving of magnetospheric ULF waves: Pulsations driven by velocity shear at the magnetopause, *J. Geophys. Res.*, *113*, A05218, doi:10.1029/2007JA012890.
- Forsyth, C., et al. (2016), What effect do substorms have on the content of the radiation belts?, *J. Geophys. Res. Space Physics*, *121*, 6292–6306, doi:10.1002/2016JA022620.
- Iles, R. H. A., A. N. Fazakerley, A. D. Johnstone, N. P. Meredith, and P. Bühler (2002), The relativistic electron response in the outer radiation belt during magnetic storms, *Ann. Geophys.*, *20*(7), 957–965, doi:10.5194/angeo-20-957-2002.
- Jaynes, A. N., et al. (2015), Source and seed populations for relativistic electrons: Their roles in radiation belt changes, *J. Geophys. Res. Space Physics*, *120*, 7240–7254, doi:10.1002/2015JA021234.
- Koons, H. C., and D. J. Gorney (1991), A neural network model of the relativistic electron flux at geosynchronous orbit, *J. Geophys. Res.*, *96*, 5549–5556, doi:10.1029/90JA02380.
- Korth, H., M. F. Thomsen, J. E. Borovsky, and D. J. McComas (1999), Plasma sheet access to geosynchronous orbit, *J. Geophys. Res.*, *104*, 25,047–25,061, doi:10.1029/1999JA900292.
- Li, L. Y., J. B. Cao, G. C. Zhou, and X. Li (2009), Statistical roles of storms and substorms in changing the entire outer zone relativistic electron population, *J. Geophys. Res.*, *114*, A12214, doi:10.1029/2009JA014333.
- Li, X. (2004), Variations of 0.7–6.0 MeV electrons at geosynchronous orbit as a function of solar wind, *Space Weather*, *2*, S03006, doi:10.1029/2003SW000017.
- Li, X., D. N. Baker, M. Temerin, D. Larson, R. P. Lin, G. D. Reeves, M. Looper, S. G. Kanekal, and R. A. Mewaldt (1997), Are energetic electrons in the solar wind the source of the outer radiation belt?, *Geophys. Res. Lett.*, *24*, 923–926, doi:10.1029/97GL00543.
- Li, X., M. Temerin, D. N. Baker, G. D. Reeves, and D. Larson (2001), Quantitative prediction of radiation belt electrons at geostationary orbit based on solar wind measurements, *Geophys. Res. Lett.*, *28*, 1887–1890, doi:10.1029/2000GL012681.
- Li, X., D. N. Baker, D. Larson, M. Temerin, G. Reeves, and S. G. Kanekal (2003), The predictability of the magnetosphere and space weather, *Eos Trans. AGU*, *84*(37), 369–370, doi:10.1029/2003EO370002.
- Li, X., D. N. Baker, M. Temerin, G. Reeves, R. Friedel, and C. Shen (2005), Energetic electrons, 50 keV to 6 MeV, at geosynchronous orbit: Their responses to solar wind variations, *Space Weather*, *3*, S04001, doi:10.1029/2004SW000105.
- Li, X., K. S. Oh, and M. Temerin (2007), Prediction of the AL index using solar wind parameters, *J. Geophys. Res.*, *112*, A06224, doi:10.1029/2006JA011918.
- Li, X., M. Temerin, D. N. Baker, and G. D. Reeves (2011), Behavior of MeV electrons at geosynchronous orbit during last two solar cycles, *J. Geophys. Res.*, *116*, A11207, doi:10.1029/2011JA016934.
- Liu, W., T. E. Sarris, X. Li, R. Ergun, V. Angelopoulos, J. Bonnell, and K. H. Glassmeier (2010), Solar wind influence on Pc4 and Pc5 ULF wave activity in the inner magnetosphere, *J. Geophys. Res.*, *115*, A12201, doi:10.1029/2010JA015299.
- Luo, B., X. Li, M. Temerin, and S. Liu (2013), Prediction of the AU, AL, and AE indices using solar wind parameters, *J. Geophys. Res. Space Physics*, *118*, 7683–7694, doi:10.1002/2013JA019188.
- Lyatsky, W., and G. V. Khazanov (2008), Effect of solar wind density on relativistic electrons at geosynchronous orbit, *Geophys. Res. Lett.*, *35*, L03109, doi:10.1029/2007GL032524.
- Mann, I. R., T. P. O'Brien, and D. K. Milling (2004), Correlations between ULF wave power, solar wind speed, and relativistic electron flux in the magnetosphere: Solar cycle dependence, *J. Atmos. Sol. Terr. Phys.*, *66*, 187–198, doi:10.1016/j.jastp.2003.10.002.
- Mathie, R. A., and I. R. Mann (2000), A correlation between extended intervals of ULF wave power and storm-time geosynchronous relativistic electron flux enhancements, *Geophys. Res. Lett.*, *27*, 3261–3264, doi:10.1029/2000GL003822.

- Mathie, R. A., and I. R. Mann (2001), On the solar wind control of Pc5 ULF pulsation power at mid-latitudes: Implications for MeV electron acceleration in the outer radiation belt, *J. Geophys. Res.*, *106*, 29,783–29,796, doi:10.1029/2001JA000002.
- Newell, P. T., T. Sotirelis, K. Liou, C.-I. Meng, and F. J. Rich (2007), A nearly universal solar wind-magnetosphere coupling function inferred from 10 magnetospheric state variables, *J. Geophys. Res.*, *112*, A01206, doi:10.1029/2006JA012015.
- O'Brien, T. P., R. L. McPherron, D. Sornette, G. D. Reeves, R. Friedel, and H. J. Singer (2001), Which magnetic storms produce relativistic electrons at geosynchronous orbit?, *J. Geophys. Res.*, *106*, 15,533–15,544, doi:10.1029/2001JA000052.
- Paulikas, G. A., and J. B. Blake (1979), Effects of the solar wind on magnetospheric dynamics: Energetic electrons at the synchronous orbit, in *Quantitative Modeling of Magnetospheric Processes, Geophys. Monogr. Ser.*, vol. 21, pp. 180–202, AGU, Washington, D. C.
- Reeves, G. D. (1998), Relativistic electrons and magnetic storms: 1992–1995, *Geophys. Res. Lett.*, *25*, 1817–1820, doi:10.1029/98GL01398.
- Reeves, G. D., K. L. McAdams, R. H. W. Friedel, and T. P. O'Brien (2003), Acceleration and loss of relativistic electrons during geomagnetic storms, *Geophys. Res. Lett.*, *30*(10), 1529, doi:10.1029/2002GL016513.
- Reeves, G. D., S. K. Morley, R. H. W. Friedel, M. G. Henderson, T. E. Cayton, G. Cunningham, J. B. Blake, R. A. Christensen, and D. Thomsen (2011), On the relationship between relativistic electron flux and solar wind velocity: Paulikas and Blake revisited, *J. Geophys. Res.*, *116*, A02213, doi:10.1029/2010JA015735.
- Rigler, E. J., M. Wiltberger, and D. N. Baker (2007), Radiation belt electrons respond to multiple solar wind inputs, *J. Geophys. Res.*, *112*, A06208, doi:10.1029/2006JA012181.
- Simms, L. E., M. J. Engebretson, V. Pilipenko, G. D. Reeves, and M. Clilverd (2016), Empirical predictive models of daily relativistic electron flux at geostationary orbit: Multiple regression analysis, *J. Geophys. Res. Space Physics*, *121*, 3181–3197, doi:10.1002/2016JA022414.
- Spence, H. E., et al. (2013), Science goals and overview of the energetic particle, composition, and thermal plasma (ECT) suite on NASA's Radiation Belt Storm Probes (RBSP) mission, *Space Sci. Rev.*, *179*, 311–336, doi:10.1007/s11214-013-0007-5.
- Temerin, M., and X. Li (2002), A new model for the prediction of *Dst* on the basis of the solar wind, *J. Geophys. Res.*, *107*(A12), 1472, doi:10.1029/2001JA007532.
- Temerin, M., and X. Li (2006), *Dst* model for 1995–2002, *J. Geophys. Res.*, *111*, A04221, doi:10.1029/2005JA011257.
- Tsyganenko, N. A. (1989), A magnetospheric magnetic field model with a warped tail current sheet, *Planet. Space Sci.*, *37*, 5–20, doi:10.1016/0032-0633(89)90066-4.
- Turner, D. L., and X. Li (2008), Quantitative forecast of relativistic electron flux at geosynchronous orbit based on low-energy electron flux, *Space Weather*, *6*, S05005, doi:10.1029/2007SW000354.
- Turner, D. L., et al. (2015), Energetic electron injections deep into the inner magnetosphere associated with substorm activity, *Geophys. Res. Lett.*, *42*, 2079–2087, doi:10.1002/2015GL063225.
- Tverskaya, L. V. (1986), On the boundary of electron injection into the magnetosphere, *Geomagn. Aeron.*, *26*(5), 864–865.
- Tverskaya, L. V., N. N. Pavlov, J. B. Blake, R. S. Selesnick, and J. F. Fennell (2003), Predicting the L-position of the storm-injected relativistic electron belt, *Adv. Space Res.*, *31*(4), 1039–1044, doi:10.1016/S0273-1177(02)00785-8.
- Vassiliadis, D., A. J. Klimas, S. G. Kanekal, D. N. Baker, and R. S. Weigel (2002), Long-term-average, solar cycle, and seasonal response of magnetospheric energetic electrons to the solar wind speed, *J. Geophys. Res.*, *107*(A11), 1383, doi:10.1029/2001JA000506.
- Wing, S., J. R. Johnson, E. Camporeale, and G. D. Reeves (2016), Information theoretical approach to discovering solar wind drivers of the outer radiation belt, *J. Geophys. Res. Space Physics*, *121*, 9378–9399, doi:10.1002/2016JA022711.
- Zhao, H., and X. Li (2013), Inward shift of outer radiation belt electrons as a function of *Dst* index and the influence of the solar wind on electron injections into the slot region, *J. Geophys. Res. Space Physics*, *118*, 756–764, doi:10.1029/2012JA018179.
- Zhao, H., et al. (2015), The evolution of ring current ion energy density and energy content during geomagnetic storms based on Van Allen Probes measurements, *J. Geophys. Res. Space Physics*, *120*, 7493–7511, doi:10.1002/2015JA021533.
- Zhao, H., et al. (2016), Ring current electron dynamics during geomagnetic storms based on the Van Allen Probes measurements, *J. Geophys. Res. Space Physics*, *121*, 3333–3346, doi:10.1002/2016JA022358.